



Electronic structure and ordering of multilayers of Co and Ag on Cu(111) investigated by photoelectron spectroscopy

J. Bork^a, L. Diekhöner^{a,*}, Z. Li^b, J. Onsgaard^a

^a Department of Physics and Nanotechnology, and Interdisciplinary Nanoscience Center (iNANO), Aalborg University, DK-9220 Aalborg, Denmark

^b Institute of Storage Ring Facilities, University of Aarhus, DK-8000 Aarhus C, Denmark

ARTICLE INFO

Article history:

Received 23 February 2010

Accepted 26 May 2010

Available online 2 June 2010

Keywords:

Multilayers

Surface state

Photoelectron spectroscopy

LEED

Cu(111)

Ag

Co

ABSTRACT

The growth and the electronic structure of multilayers of Co and Ag on Cu(111) at room temperature have been studied with photoelectron spectroscopy and low-energy electron diffraction (LEED). The coverage range spans from Co and Ag layers between one monolayer (ML) to stacking of several monolayers. Surface states and ordered structures have been identified at room temperature. A Ag-related surface state with a binding energy of 0.30 eV is identified in normal emission in the ultraviolet photoelectron spectra when silver constitutes the top layer. Core-level binding energy shifts of Ag 3d_{5/2} reflect the changing surroundings of Ag. Hexagonal diffraction patterns are observed for sandwiches of consecutive layers of Co and Ag up to 5 layers. Since no interlayer diffusion is observed in the layer-by-layer formation of the films, multilayers of consecutive silver and cobalt on Cu(111) offer preparation of sandwiched magnetic–non-magnetic structures.

© 2010 Elsevier B.V. All rights reserved.

1. Introduction

Multilayers of ultrathin metallic films grown on top of a metallic substrate can exhibit new physical and chemical properties compared to those characteristic of the bulk. Surface relaxation, superstructures, induced strain and the reduced dimensionality are among the phenomena that influence the electronic structure of the multilayer films and the interfaces. Catalysis and magnetism are currently active research fields where newfound effects can be beneficial for processes and devices [1,2].

Ultrathin films made of alternating layers of magnetic and nonmagnetic metals can exhibit oscillatory magnetic coupling and the giant-magnetoresistance effect [3–5]. Variation of the magnetic properties of ultrathin films of Co on metal substrates and the effect of introducing a cap of a noble metal has been much studied. Araki et al. [6] reported on a large and oscillating magnetoresistance in evaporated Ag/Co multilayers and Loloee et al. confirmed these observations [7]. Kohlhepp et al. observed that whereas the free Co(0001) surface supports in-plane magnetization, capping with Ag supports perpendicular magnetization with a maximum in the magnitude of magnetic surface anisotropy for 1 monolayer (ML) Ag [8]. It was found by Chen et al. that 1 ML of Ag deposited on a Co(5ML)/Pt surface causes a reorientation of the easy axis of the magnetization from the in-plane to the out-of-plane direction [9]. Tsay et al. studied the var-

iation of the magnetic properties of Co/Cu(111) films upon Ag deposition up to a few ML and observed a Ag overlayer-induced oscillation of the coercive force as the thickness of the Ag overlayer increases [10]. Noble metal capping effects on the spin-reorientation transitions of Co/Ru(0001) were studied by El Gabaly et al., who found that the noble metal capping results in spin-reorientation transitions that depend on the atomic layer thickness of the capping layer [11].

Accordingly, there is a need for a detailed understanding of the geometrical and the electronic structures of multilayer films consisting of a magnetic metal and a noble metal capping, from the sub-monolayer coverage to thicknesses of the order of a few nanometers.

There is a substantial amount of literature on the electronic and morphological structures of ultrathin Co layers on Cu(111). The reports on the electronic structure include photoemission [12,13] and inverse photoemission measurements [14], quantitative low-energy electron diffraction (LEED), photoelectron diffraction and Fermi surface mapping of Co/Cu(111) [15–17]. Furthermore, scanning tunneling spectroscopy (STS) was used for the study of the electronic structure around the Fermi level [18,19].

The room-temperature growth of Co on Cu(111) in the low-coverage regime, $\theta < 2$ ML, is characterized by the formation of islands of triangular shape and bilayer height above the Cu(111) surface [20,21]. With increasing coverage, single layers of Co grow on top of the Co islands and 3-dimensional growth is observed [20]. The ultrathin Co film is dominated by continuation of the fcc stacking dictated by the copper [22]. A 5 ML thick Co film exhibits a hexagonally close-packed structure [23].

* Corresponding author.

E-mail address: ld@nano.aau.dk (L. Diekhöner).

Recently the initial stages of the room-temperature growth of Ag on bilayer high Co nanoislands on Cu(111) have been studied by scanning tunneling microscopy (STM) [24]. It was found that there is a preferred nucleation for Ag on top of Co compared to Cu(111) terrace sites at low Ag doses. Furthermore, it was observed that the Co islands are either completely free of Ag or completely capped with Ag. The Ag adlayer formed a 9×9 reconstruction due to the lattice mismatch [24]. When the Ag coverage increases above ca 1 ML there is no particular preference and the Ag simply grows layer by layer as seen for Ag on Cu(111) [25]. In a recent STS-study, it was shown how the deposition of Ag on Co/Cu(111) modulates the electronic landscape around the Fermi level of the heterostructured interface. By spectroscopic mapping of the local density of states it was observed that a modulation of the energy position, width and intensity of the Co d-state is correlated with the morphology of the silver Moiré pattern [26].

The purpose of the present report is to characterize the electronic structure of multilayers, consisting of the magnetic element, Co, and the noble metal, Ag, on the Cu(111) surface in the coverage range of 1 ML to 8 ML. It is found that the successive build up of the layers at room temperature takes place without interlayer diffusion. LEED shows ordering and a Ag associated surface state is identified when Ag forms the topmost layer. The experimental evidence is based on photoelectron spectroscopy in the form of core-level spectroscopy (CLS) and energy distribution curves (EDCs) of the valence electrons.

2. Experimental

The experiments were performed in an ultrahigh-vacuum (UHV) chamber, with a base pressure $< 4 \times 10^{-8}$ Pa, attached to the SGM1/Scienta beamline at the storage ring ASTRID at Aarhus University. The beamline consists of a spherical grating monochromator and the end-station is equipped with a hemispherical Scienta SES-200 electron energy analyzer and a channelplate as a detector. The photon beam incidence angle was 40° relative to the sample normal and the spectra were collected with the electron emission parallel to the normal of the surface. Concerning the EDCs of the valence band (VB) electrons and the Ag $3d_{5/2}$ core electrons, the total instrumental resolution was better than 100 meV and 300 meV, respectively. VB EDCs were recorded either in a small-angle mode with an analyzer acceptance angle of $\pm 1^\circ$ or in an integral mode with an acceptance angle of $\pm 9^\circ$. Further, X-ray photoelectron spectroscopy (XPS) could be performed via a Mg- K_α X-ray source in connection with the analyzer. The X-ray tube was thoroughly degassed. A LEED facility allows detection of ordered overlayer structures. Cleaning of the Cu sample was carried out by repeated cycles of Ar^+ sputtering followed by annealing at $500^\circ C$. Overlayers of Ag were prepared by evaporation from an electron bombarded crucible and Co was evaporated by electron bombardment from a high-purity Co wire; the Cu(111) sample was kept at room temperature. The Co flux was 0.22 ML/min and the deposition rate of Ag was 0.24 ML/min. Calibrations of the sources were carried out using the photoemission intensities versus dose curves and an oscillating quartz crystal thickness monitor. The cleanliness of the samples was assessed by checking that the C and O 1s signals were below the noise level. A further sensitive check of the surface purity, before and after recording of the UPS and XPS measurements, was the non-presence of the CO 4 signal in the valence band spectrum. The photoemission spectra were recorded at room temperature. The angular resolution is estimated to be 0.5° corresponding to a k -resolution of 0.020 \AA^{-1} for a photon energy of 40 eV. Alignment of the sample normal and the spectrometer was performed via the LEED apparatus. STM experiments have been performed in a different UHV-system as described in [24]. We note that the same metal-evaporator was used in both systems making it easier to compare and calibrate doses.

In the following the compositions of the multilayers on the Cu(111) substrate are written as $Ag(m)/Co(n)/Cu(111)$ where m and n

indicate the number of Ag and Co monolayers, respectively, deposited on the Cu(111) surface, here with Co as the first deposit material. The term monolayer is used as the atomic amount deposited. Analysis and fitting of the core-level spectra of Cu $2p_{3/2}$, Co $2p_{3/2}$ and Ag $3d_{5/2}$ were based on a Doniach–Sunjic line shape [27] convoluted with a Gaussian distribution function using the program FitXPS [28].

3. Results and discussion

3.1. Growth curves

Co was evaporated on Cu(111) at room temperature and the growth was followed using CLS of Cu $2p_{3/2}$ and Co $2p_{3/2}$. The growth curves shown in Fig. 1 exhibit linear segments, where the Cu $2p_{3/2}$ curve has a knee-point at 2.7 ML Co and the Co $2p_{3/2}$ curve has a less pronounced cutting point at 2.4 ML Co. Thus, keeping the island growth of Co in mind, the break points on the growth curves, corresponds to an almost fully covered Cu(111) surface. This is corroborated by STM images (Fig. 1), which have been recorded in a different UHV-system using the same doses of Co. It was found that the STM image with a cobalt coverage of $\theta_{Co} = 2.2$ ML corresponds to a 15% free copper substrate. From the intensity decay curve of Cu $2p_{3/2}$ a reduction in intensity to 53% of the intensity of the uncovered surface is read at this Co coverage. This number can be compared with the intensity reduction estimated in a simplistic attenuation model where the measured Cu 2p intensity is a sum of the contribution from the free Cu surface (15%) and the contribution from the Co covered part. According to the STM results (Fig. 1) the Co covered part of the surface is characterized by mostly bilayer (3.9 Å high) islands as well as some in the third layer. The attenuation of the Cu 2p intensity by passage of the 2.2 ML Co is determined by the electron mean free path in the Co layers, which is $\lambda_{Co} = 3.0$ ML for electrons with a kinetic energy of

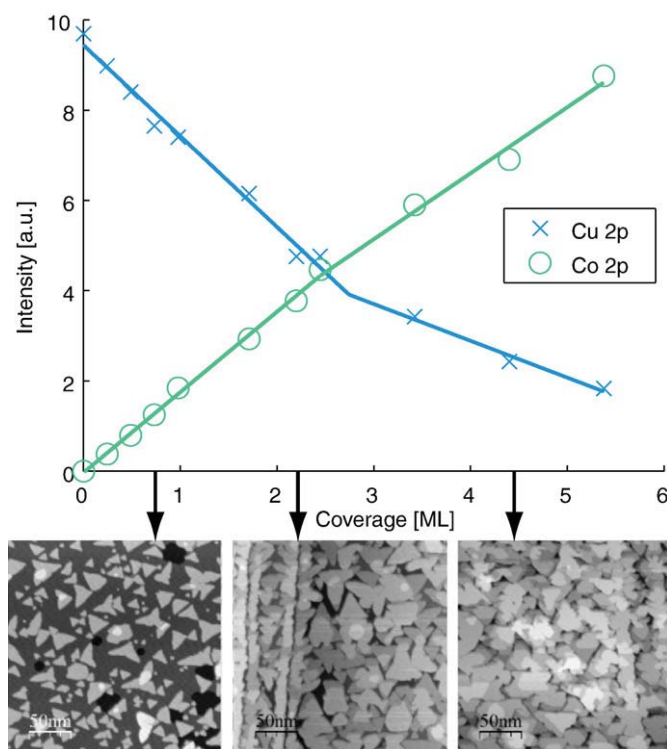


Fig. 1. The evolution of the Co $2p_{3/2}$ and Cu $2p_{3/2}$ intensities as a function of deposited cobalt. In order to correlate photoelectron data and STM results for the same system three STM inserts, recorded for coverages of 1.1, 2.2 and 4.4 ML Co, show the evolution of the triangular Co islands distributed on the Cu(111) terraces. Note that initially the visible coverage of the Cu(111) surface with bilayer islands of Co is half the deposited amount.

320 eV as is the case for 2p-electrons emitted from the copper substrate [29]. This results in a Cu 2p_{3/2} intensity reduction of 55% in good agreement with the attenuation in intensity found above.

To visualize the effect of adding Ag we show in Fig. 2A an STM image of 0.5 ML Ag deposited on a Cu(111) surface pre-covered with 0.25 ML Co. The majority of the islands are covered with Ag (seen as the bright islands in the image). Furthermore Ag is also seen to nucleate on Cu(111) at the step edges. At lower Ag coverage the Ag-capping of Co islands is even more pronounced such that the Ag initially mainly is observed on the Co islands and only very little on the Cu terraces. For details we refer to Ref. [24]. Relevant for the studies shown here we show in Fig. 2B an STM image of 2.2 ML Ag on 0.7 ML Co/Cu(111). The triangular Co islands are still visible through the Ag layer due to the topographic height difference of Ag and Co (see also the schematic inset of Fig. 4).

3.2. Ag 3d_{5/2} core-level spectra for Ag/Co/Cu(111)

Next Ag is evaporated on a Co pre-covered Cu(111) sample at room temperature and Ag 3d_{5/2} EDCs are measured. The Co coverage was kept constant at 0.66 ML whereas the Ag coverage ranged from 0.75 ML to 2.0 ML. The spectra (Ag 3d_{5/2}) are shown in Fig. 3. It is observed that the Ag 3d_{5/2} peaks have more than one component reflecting that different surroundings of the silver atoms result in a chemical shift. A decomposition of the peak for $\theta_{Ag} = 0.75$ ML results in a low-binding energy component, $E_{B,L}$ at 367.70 eV and a high-binding energy component, $E_{B,H}$ at 368.03 eV. For comparison a Ag (0.7ML)/Cu(111) interface, without Co, with silver was prepared at room temperature. The Ag 3d_{5/2} curve is displayed as the lower curve in Fig. 3, showing an $E_B = 367.87$ eV. This finding supports an interpretation of silver mostly occupying the top of the Co islands [24]. For the Ag/Cu(111) interface an increasing E_B for Ag 3d_{5/2} with increasing silver coverage was observed corresponding to +270 meV for the 3.3 ML thick silver film. The present determined binding energy $E_B = 368.15$ eV for the 3.3 ML thick Ag film coincides with the Ag bulk $E_B = 368.19$ eV determined by Citrin et al. [30] and it is close to the $E_B = 368.00$ eV for a 20 ML Ag film deposited on Ru(0001) measured by Rodriguez [31]. In Ref. [32] it was reported that the surface core-level shift in Ag(111) is below 100 meV.

Deposition of different amounts of Ag on a Co(2.2ML)/Cu(111) surface at room temperature results in the Ag 3d_{5/2} spectra shown in Fig. 4. A fitting procedure based on a single peak approach gives rise to a Lorentzian line-width around 0.36 eV and a Gaussian line-width around 0.39 eV. It is seen, taking the uncertainty in the energy determination into consideration, that E_B is constant, 368.05 eV. This observation is on line with the STM findings in Ref. [24] where the silver caps the bilayer high cobalt islands. Another observation from the present results is the constancy of E_B for Ag 3d_{5/2} with θ_{Ag} above 1 ML.

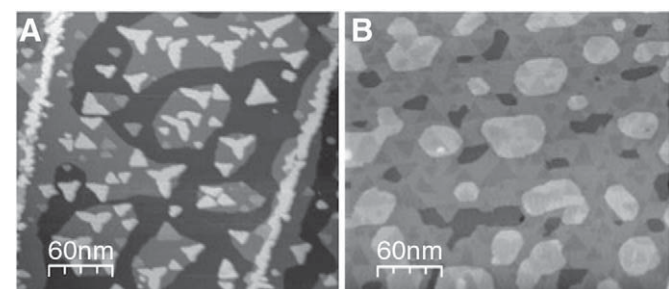


Fig. 2. A) STM image of 0.5 ML Ag on 0.5 ML Co/Cu(111). B) STM image of 2.2 ML Ag on 0.7 ML Co/Cu(111).

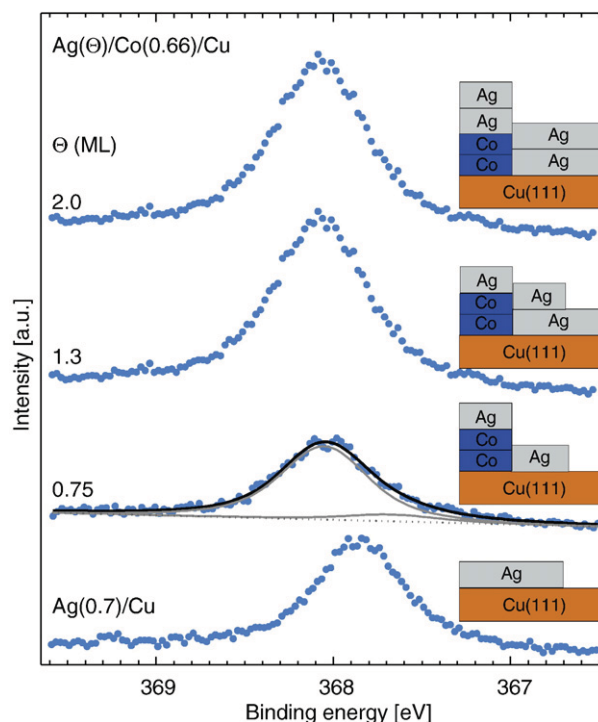


Fig. 3. The bottom curve shows a Ag 3d_{5/2} core-level spectrum for 0.7 ML of Ag deposited on a Cu(111) surface at room temperature. The next three curves display Ag 3d_{5/2} spectra for 0.75 ML, 1.3 ML and 2.0 ML of Ag deposited on a Co(0.66 ML)/Cu(111) interface at room temperature. A decomposition of the spectrum for 0.75 ML Ag is included. The photon energy was 435 eV. Simple model images of the structures are shown on the right hand side. These are based on the STM results of Ref. [24], but are only very schematic for simplicity.

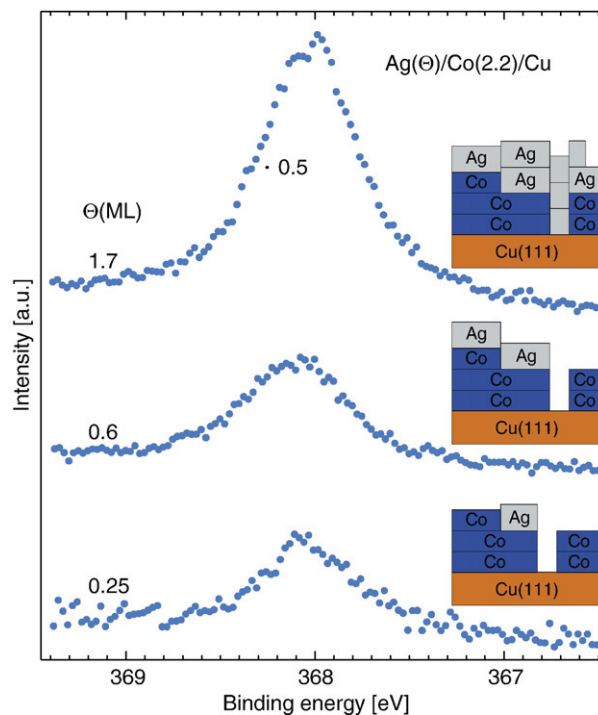


Fig. 4. Ag 3d_{5/2} core-level spectra for different coverages of Ag on a Co(2.2ML)/Cu(111) interface. From bottom and upwards the Ag coverages are 0.25 ML, 0.6 ML and 1.7 ML. The photon energy was 435 eV. Schematic images of the structures are also shown.

3.3. Valence band energy distribution curves, integral and small-angle measurements

Valence band EDCs for multilayer films recorded in the integral mode, shown in Figs. 5–7, clearly illustrate that the VB energy range is divided in intervals representing Co, Cu and Ag, as read from the Fermi edge. All overlayers were formed at room temperature and the VB spectra were recorded for incoming photon energy of 40 eV. At this photon energy the cross sections for the 3d electrons of Co and Cu, and the 4d electrons of Ag are 8.7, 9.9 and 38 Mbarn, respectively [33]. Deposition of 2.2 ML Co on the Cu(111) substrate gives rise to the EDC shown in Fig. 5 as the upper curve (i). A 2 eV broad structure with a maximum E_B of 0.50 eV occurs near the Fermi level well separated from the Cu 3d main structure. Alkemper et al. observed maximum intensity at $E_B = 0.7$ eV for 1.7 ML Co on Cu(111) in normal emission and $h\nu = 25$ eV [13]. Addition of 1.7 ML Ag changes the density of states (DOS) in the low-binding energy range with a shift of the maximum towards lower E_B , curve (ii). The changes are observable in the difference curve, (ii)–(i), where a small structure at the Fermi level indicates a Ag induced surface or interface state. The negative excursions in the E_B -ranges, 0.2–1.5 eV, and 2–3 eV, reflect the damping influence of the Ag layers on the photoelectron intensity from the underlying Co and Cu layers.

The effects of adding a 2.2 ML thick Co layer on top of a Ag(1.8ML)/Co(2.2ML)/Cu(111) interface are demonstrated in Fig. 6, where we show valence band curves for Ag(1.8ML)/Co(2.2ML)/Cu(111) and Co(2.2)/Ag(1.8ML)/Co(2.2ML)/Cu(111) together with the difference curve. Co 3d constitutes the VB in the E_B -range 0–2 eV, and the surface state due to Ag is removed when Co constitutes the top layer. For E_B 's higher than 2 eV the difference spectrum is negative reflecting the attenuation of photoelectrons originating from the Ag and Cu subsurface layers.

In Fig. 7 we present valence band spectra of a sample prepared with varying Co coverages and constant Ag coverage. The three upper EDCs in Fig. 7 are dominated by Ag, and the Cu(111) substrate is hardly recognizable in the two upper spectra where 6 overlayers are present. In the case of a submonolayer coverage of Co, the lowest curve in Fig. 7, the EDC exhibits pronounced contributions from Ag and the Cu substrate. Thus, the attenuation of the Cu 4d spectrum, and further, the relative intensities of Co and Ag demonstrate that interlayer mixing does not take place in any significant way. Again, the evolution of the EDC close to the Fermi level, $0 \text{ eV} < E_B < 2 \text{ eV}$, is

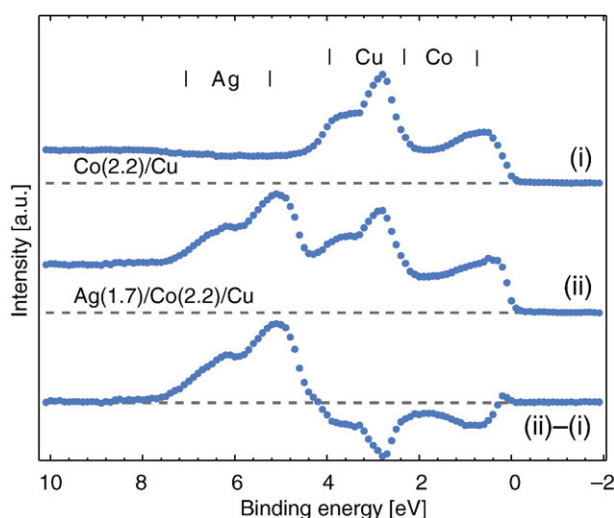


Fig. 5. Valence band spectra obtained with photons of energy 40 eV. The upper spectrum, (i), represents an interface with 2.2 ML Co deposited on Cu(111) at room temperature. Next spectrum, (ii), displays the VB spectrum after deposition of 1.8 MLs of Ag at room temperature and the lowest curve shows the difference spectrum, (ii)–(i).

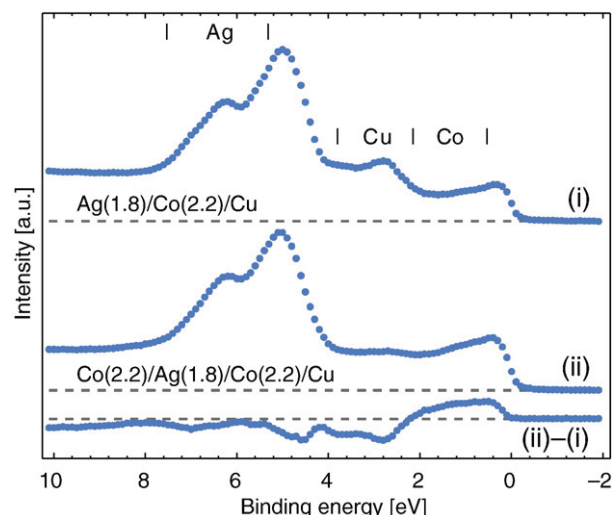


Fig. 6. Valence band spectra demonstrating the effect of adding 2.2 ML Co to a sandwich consisting of Ag(1.8)/Co(2.2)/Cu(111). Co 3d becomes the dominant component in the structure near the Fermi level and the maximum intensity is observed at a 100 meV higher E_B .

informative. For the interface spectrum, shown as the bottom curve, with a low Co coverage, 0.4 ML, the band is flat in contrast to curve two and three from below, where 2.2 ML of Ag is deposited on 2.2 and 4.4 ML of Co, respectively. A maximum in the EDC is observed at an increasing E_B due to the growing influence of Co. For 2.2 ML Ag embedded in 2 ML thick Co layers, the maximum is shifted to a E_B which is 0.18 eV compared to that characteristic of the Ag(2.2ML)/Co(4.4ML)/Cu(111) interface.

To summarize the integral measurements of the VB EDCs it is deduced that the layers grow as deposited at room temperature and a Ag-related surface state on Ag(1.8)/Co(2.2)/Cu(111) can be assigned.

3.4. Small-angle photoemission and LEED

We now reduce the acceptance angle of the detector from $\pm 9^\circ$ to $\pm 1^\circ$. The normal emission spectra, $\theta = 0$, for the Ag(2.2)/Co(0.4)/

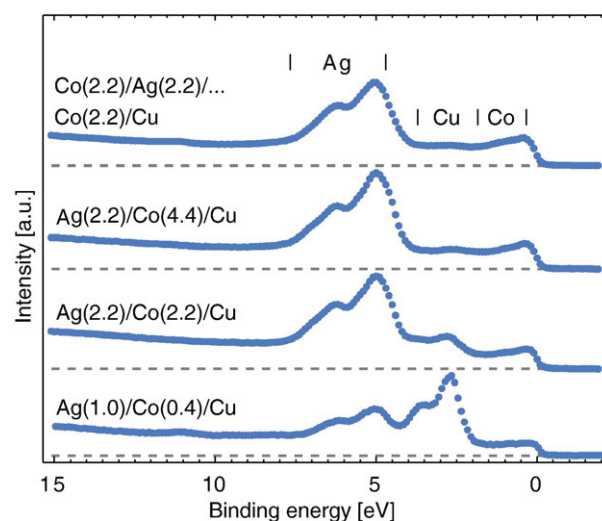


Fig. 7. Valence band PES spectra of multilayers of Ag and Co, deposited on Cu(111) at room temperature, obtained with a photon energy of 40 eV. From below, the spectrum is recorded from a Cu(111) surface after deposition of 0.33 ML Co and further deposition of 1.0 ML Ag. The next two spectra are recorded for 2.2 and 4.4 ML of Co covered with 1.0 and 2.2 ML of Ag, respectively. A VB spectrum of a 6 ML sandwich of changing Co and Ag is displayed as the upper curve.

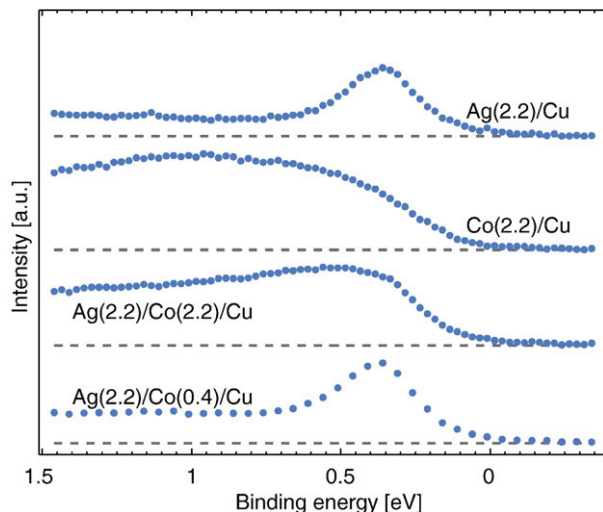


Fig. 8. Small-angle photoemission spectra in normal emission recorded with a photon energy of 40 eV. Spectra of one-component overlayers with Ag and Co on the substrate are shown as the two upper curves. EDCs of sandwiches with 2.2 ML Ag as the top layer and different Co coverages of 0.4 ML and 2.2 ML as the intermediate layer are shown as the lowest and next-lower curves, respectively.

Cu(111) surface and the Ag(2.2)/Cu(111) surface are shown in Fig. 8 as the lowest curve and the top curve, respectively. Compared to the Ag(2.2)/Cu(111) spectrum a slightly increased intensity for binding energies higher than 0.4 eV is observed in the Ag(2.2)/Co(0.4)/Cu(111) spectrum. This is due to the presence of the bilayer Co islands. Thus, the photoemission spectrum of the last mentioned surface is composed of contributions partly from areas where Cu(111) is covered by Ag and partly from areas where bilayer high Co islands are covered by Ag.

It is instructive to observe the effect of adding 2.2 ML of Ag on the photoemission spectra of a Cu(111) surface covered with 2.2 ML of Co, where the spectra are recorded in normal emission (see Fig. 8). The spectrum of the Co(2.2)/Cu(111) surface, second curve from above, is characterized by a broad feature with a maximum at 0.8 eV and a broad shoulder around 0.5 eV. The Co(2.2)/Cu(111) spectrum shows much resemblance to the angular-resolved EDC of photoelectrons using s-polarized light for the Co(2.2)/Cu(111) interface reported in Ref. [12]. As determined from spin-resolved photoemission spectra the Co 3d emission peak positioned close to the Fermi level is a composite of spin-up and spin-down photoelectrons [13]. For a coverage of 2.8 ML Co on Cu(111), a photon energy of 25 eV and normal emission, the spin-up and spin-down emission peak at 0.80 eV and the spin-up electrons exhibited a slow decay at higher binding energies.

The deposition of 2.2 ML of Ag on top of Co(2.2)/Cu(111), the third curve from above, causes a strong change of the spectrum with an energy shift towards the Fermi level and a broad peak around a binding energy of 0.30 eV. A difference spectrum (not shown), formed by subtraction of the Co(2.2)/Cu spectrum from the Ag(2.2)/Co(2.2)/Cu spectrum, displays a narrow peak at 0.3 eV binding energy and a broad negative excursion with a minimum at 0.9 eV binding energy. These energy positions confirm that the composite spectrum can be interpreted as a superposition of the Ag component in the uppermost layer and the Co component beneath the surface layer.

For a 2.2 ML thick Ag film on a Co(4.4)/Cu(111) substrate we observe a state with a binding energy of 0.30 \pm 0.05 eV (Fig. 9, lower curve). Increasing the amount of Ag on top (from 2.2 to 4.4 ML) leads to a reduction in binding energy by ca 0.15 eV (comparing the two lower spectra in Fig. 9). Similar observations have been done for Ag layers on Cu(111), where increasing amounts of Ag also reduced the binding energy of the surface state [34]. Finally, for a double Ag–Co

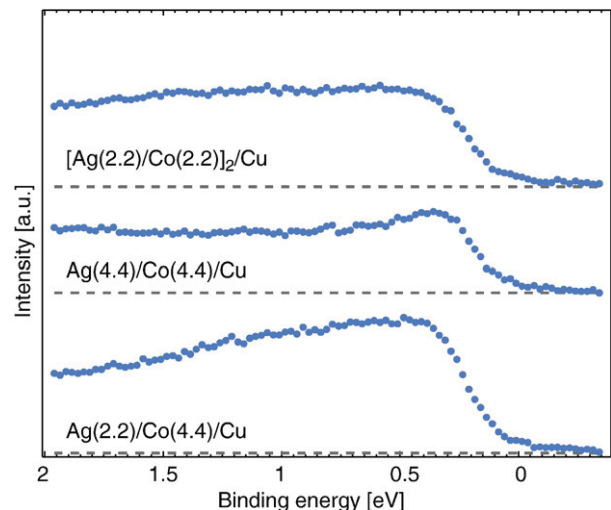


Fig. 9. Small-angle photoemission spectra in normal emission recorded with a photon energy of 40 eV. The two lower curves show Ag/Co/Cu with fixed Co coverage and an increasing amount of Ag on top. The topmost curve shows a spectrum of a double sandwich with alternating Co and Ag layers.

sandwich film, the upper curve in Fig. 9, the peak at 0.30 eV E_B is not clearly present anymore.

We interpret the state discussed above as the lower band apex of a parabolic free-electron-like surface state related to the Ag layer. Similar observations have been reported for Ag layers on Cu(111), where Bendouan et al. studied the evolution of the surface state of Ag ultrathin films on Cu(111) and observed a surface feature at 0.19 eV in the normal emission spectrum [35]. Wessendorf et al. observed a state at 0.230 eV for 1 ML Ag on Cu(111) that exhibited further shifts with increasing layer thickness [34]. The binding energy of the surface state on the thin Ag film on Cu(111) thus lies in between the value for clean Cu(111) and clean Ag(111), which support surface states with binding energies of 0.435 eV and 0.065 eV respectively (Ref. [36] and references therein). The state on the Ag adlayer thus gradually moves to the value of the pure Ag(111) state. In agreement with these observations we find that a thicker Ag layer leads to an upshift of the state.

At this point we should mention the state observed in scanning tunneling spectroscopy of Ag/Co/Cu(111) [26]. This was measured at an energy of ca 0.2 eV below the Fermi level and thus in the same range as the state we observe here in photo emission. But the nature of the state was different since it was assigned to a *d*-related surface state originating from the Co layer. The later has been very clearly seen by low-temperature STS [18], but not by room-temperature photoemission experiments [13]. We therefore believe that the state we observe is not related to the Co *d*-state but is rather a free-electron-like Shockley type surface state related to the Ag layer. This is also supported by the fact that we observe the state also for rather thick (4 ML) Ag layers, which would lead to a significant damping of the state if it would originate from the Ag–Co interface. This is in contrast to our findings.

In Fig. 10 we present a sequence of LEED patterns of Co(2.2)/Cu(111), Ag(2.2)/Co(2.2)/Cu(111), Co(2.2)/Ag(2.2)/Co(2.2)/Cu(111) and Ag(2.2)/Co(2.2)/Ag(2.2)/Co(2.2)/Cu(111). The primary kinetic energy (E_p) of incident electrons was in the range 115–143 eV (see figure caption for details). For 2.2 ML Co on Cu(111) we observe a LEED image (Fig. 10A) with hexagonal structure originating from the Cu(111) substrate and the Co islands, which grow pseudomorphically on the Cu(111) surface. Addition of two layers of Ag results in an image (Fig. 10B) that agrees with the pattern measured in Ref. [24] exhibiting a 6-spot pattern, where each spot is surrounded by 6 satellites due to the Ag overlayer, which forms a (9 \times 9) reconstruction

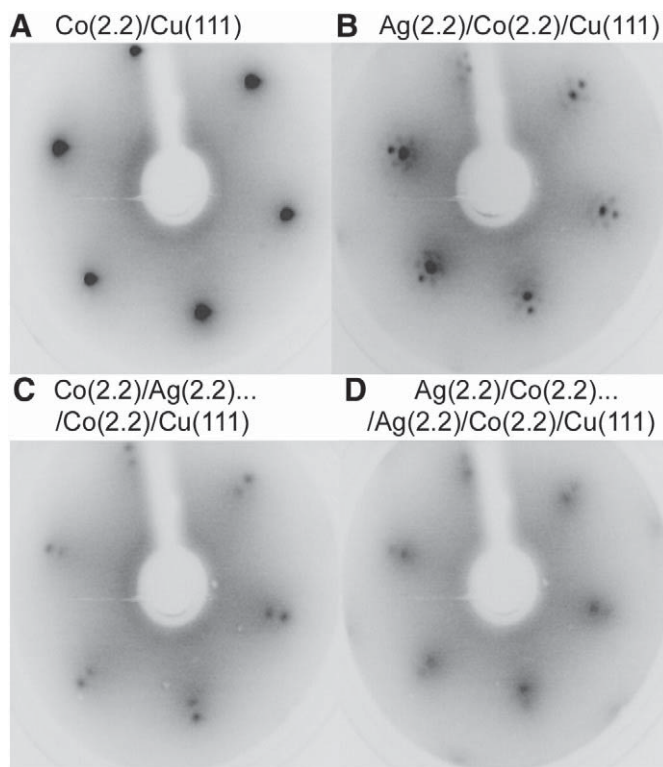


Fig. 10. LEED images from a series of multilayers deposited at room temperature on Cu(111). (A) represents Co(2.2)/Cu(111) recorded with $E_p = 136$ eV; (B) Ag(2.2)/Co(2.2)/Cu(111) with $E_p = 115$ eV; (C) Co(2.2)/Ag(2.2)/Co(2.2)/Cu(111) with $E_p = 121$ eV and (D) Ag(2.2)/Co(2.2)/Ag(2.2)/Co(2.2)/Cu(111) with $E_p = 143$ eV.

due to lattice mismatch. A well-ordered sandwich, as judged by LEED, is thus obtainable. Further deposition of 2.2 ML Co at room temperature (Fig. 10C) gives rise to two concentric and hexagonal patterns with a 9% change in distance from the (00) beam. We assign the inner spots to Cu and the outer spots to Co. Apparently, the topmost Co layer is ordered but exhibits a different lattice constant than the Cu substrate (compare with Fig. 10A). Finally, repeated deposition of 2.2 ML Ag (Fig. 10D) leads to an increasing diffusivity, reflecting that no diffraction ordering occurs in the last deposited Ag layer.

It is important to emphasize that the layers grow with no apparent intermixing or segregation. There are several observations supporting this statement. The STM experiments (see Fig. 2 and Ref. [24,26]) demonstrate that the layers grow in a well-ordered way without intermixing. This is in particular seen in the atomic-resolution STM images recorded at low temperatures (6 K) [26]. Surface free energy arguments support that Ag prefers to form a compact film on Co without segregation [24]. For Co deposited on top of Ag/Co/Cu(111) the surface free energy should be reduced if Co segregates into the bulk leaving Ag at the surface-vacuum interface. But we would then observe the 9×9 reconstruction in the LEED experiment, which apparently is not the case at room temperature (see Fig. 10C) and we thus conclude that Co stays on top. The LEED data in general show that the overall hexagonal crystalline structure is preserved and rules out irregular intermixing or alloying. This is also supported by the discussion related to the data in Fig. 7, where the addition of overlayers leads to damping of photoelectrons from lower lying layers. From the EDC-curves in Fig. 9 we conclude that the addition of Co to Ag/Co/Cu(111) leads to a quenching of the Ag-related state — again in favor of Co staying on top.

4. Conclusions

In conclusion, multilayers of Co and Ag deposited on a Cu(111) substrate at room temperature have been characterized in terms of electronic structure and ordering. In combination with a recent work on the growth and atomic structure of Ag on bilayer Co nanoislands on Cu(111) [24] the following picture emerges. It is possible to prepare sandwiched magnetic-nonmagnetic Co–Ag structures. The E_B of Ag $3d_{5/2}$ is sensitive to the surroundings of the Ag causing a core-level shift between Ag positioned on top of Co and Ag covering free Cu sites. Valence band energy distribution curves for consecutive layers of Co and Ag show layer-by-layer growth and exhibit a Ag associated surface state when Ag is the last deposited component. The binding energy of the surface state is 0.30 eV for the Ag(2.2)/Co(0.4)/Cu(111), the Ag(2.2)/Co(2.2)/Cu(111) and the Ag(2.2)/Co(4.4)/Cu(111) sandwiches. It is demonstrated by LEED that the structures are well-ordered. The Ag(m)/Co(n)/Cu(111) multilayer system has a potential for magnetic studies of Co embedded between noble metals even at room temperature.

References

- [1] G. Ertl, H. Knözinger, F. Schüth, and J. Weitkamp, *Handbook of Heterogeneous Catalysis*, 2. ed. 2008; Wiley.
- [2] J. Stöhr, H. Siegmann, *Magnetism: From Fundamentals to Nanoscale Dynamics* Springer Series in Solid State Sciences, Vol. 152, Springer, Berlin, 2006.
- [3] M.N. Baibich, J.M. Broto, A. Fert, F.N.V. Dau, F. Petroff, P. Eitenne, G. Creuzet, A. Friederich, J. Chazelas, *Phys. Rev. Lett.* 61 (1988) 2472.
- [4] G. Binasch, P. Grünberg, F. Saurenbach, W. Zinn, *Phys. Rev. B* 39 (1989) 4828.
- [5] M.D. Stiles, *Phys. Rev. B* 48 (1993) 7238.
- [6] S. Araki, K. Yasui, Y. Narumiya, *J. Phys. Soc. Jpn.* 60 (1991) 2827.
- [7] R. Loloee, P.A. Schroeder, W.P. Pratt Jr., J. Bass, A. Fert, *Physica B* 204 (1995) 274.
- [8] J. Kohlhepp, U. Gradmann, *J. Magn. Magn. Mater.* 139 (1995) 347.
- [9] F.C. Chen, Y.E. Wu, C.W. Su, C.S. Shern, *Phys. Rev. B* 66 (2002) 184417.
- [10] J.S. Tsay, J.Y. Lin, C.S. Yang, Y.D. Yao, Y. Liou, *Surf. Sci.* 482–485 (2001) 1040.
- [11] F.E. Gabaly, K.F. McCarty, A.K. Schmid, J.d.I. Figuera, M.C. Munoz, L. Szunyogh, P. Weinberger, S. Gallego, *New J. Phys.* 10 (2008) 073024.
- [12] R. Miranda, F. Ynduráin, D. Chandesris, J. Lecante, Y. Petroff, *Phys. Rev. B* 25 (1983) 527–530.
- [13] U. Alkemper, C. Carbone, E. Vescovo, W. Eberhardt, O. Rader, W. Gudat, *Phys. Rev. B* 50 (1994) 17496–17501.
- [14] G.J. Mankey, R.F. Willis, F.J. Himpsel, *Phys. Rev. B* 47 (1993) 190–196.
- [15] K. Heinz, S. Müller, L. Hammer, *J. Phys. Condens. Matter* 11 (1999) 9437–9454.
- [16] V. Scheuch, K. Potthast, B. Voigtländer, H.P. Bonzel, *Surf. Sci.* 318 (1994) 115–128.
- [17] J. Osterwalder, T. Greber, E. Wetli, J. Wider, H.J. Neff, *Prog. Surf. Sci.* 64 (2000) 65–87.
- [18] L. Diekhöner, M.A. Schneider, A.N. Baranov, V.S. Stepanyuk, P. Bruno, K. Kern, *Phys. Rev. Lett.* 90 (2003) 236801.
- [19] O. Pietzsch, A. Kubetzka, M. Bode, R. Wiesendanger, *Phys. Rev. Lett.* 92 (2004) 057202.
- [20] J.d.I. Figuera, J.E. Prieto, C. Ocal, R. Miranda, *Phys. Rev. B* 47 (1993) 13043–13046.
- [21] N.N. Negulyaev, V.S. Stepanyuk, P. Bruno, L. Diekhöner, P. Wahl, K. Kern, *Phys. Rev. B (Condens. Matter Materials Phys.)* 77 (2008) 125437.
- [22] J.d.I. Figuera, J.E. Prieto, G. Kostka, S. Müller, C. Ocal, R. Miranda, K. Heinz, *Surf. Sci.* 349 (1996) L139–L145.
- [23] C. Rath, J.E. Prieto, S. Müller, R. Miranda, K. Heinz, *Phys. Rev. B* 55 (1997) 10791–10799.
- [24] J. Bork, J. Onsgaard, L. Diekhöner, *J. Phys. Condens. Matter* 22 (2010) 135005.
- [25] W.E. McMahon, E.S. Hirschorn, T.C. Chiang, *Surf. Sci.* 279 (1992) L231.
- [26] J. Bork, P. Wahl, L. Diekhöner, K. Kern, *New J. Phys.* 11 (2009) 113051.
- [27] S. Doniach, M. Sunjic, *J. Phys. C* 3 (1970) 285.
- [28] D.L. Adams, *FitXPS: Aarhus University*.
- [29] M.P. Seah, W.A. Dench, *Surf. Interface Anal.* 1 (1979) 2.
- [30] P.H. Citrin, G.K. Wertheim, Y. Baer, *Phys. Rev. B* 27 (1983) 3160.
- [31] J.A. Rodriguez, *Surf. Sci.* 296 (1993) 149.
- [32] J.N. Andersen, D. Hennig, E. Lundgren, M. Methfessel, R. Nyholm, M. Scheffler, *Phys. Rev. B* 50 (1994) 17525.
- [33] J.J. Yeh, I. Lindau, *At. Data Nucl. Data Tables* 32 (1985) 1.
- [34] M. Wessendorf, C. Wiemann, M. Bauer, M. Aeschlimann, M.A. Schneider, H. Brune, K. Kern, *Appl. Phys. A* 78 (2004) 183.
- [35] A. Bendounan, H. Cercellier, Y. Fagot-Ruvurat, B. Kierren, V.Y. Yurov, D. Malterre, *Phys. Rev. B* 67 (2003) 165412.
- [36] F. Reinert, G. Nicolay, S. Schmidt, D. Ehm, S. Hüfner, *Phys. Rev. B* 63 (2001) 115415.